

Weak Boson Production Amplitude Zeros; Equalities of the Helicity Amplitudes

Fizuli Mamedov

Department of Physics, State University of New York, Buffalo, New York 14260

Abstract. We investigate the radiation amplitude zeros exhibited by many Standard Model amplitudes for triple weak gauge boson production processes. We show that $WZ\gamma$ production amplitudes have especially rich structure in terms of zeros, these amplitudes have zeros originating from several different sources. It is also shown that TYPE I current null zone is the special case of the equality of the specific helicity amplitudes.

I INTRODUCTION

The SM amplitudes for processes with the neutral gauge boson(s) emission exhibit zeros. Either the distribution of the scattering angle contains zeros, or the helicity amplitudes completely vanish for certain polarization (or momentum) combinations of the particles which participate in the process. In this work we review the theoretical basis of these radiation amplitude zeros, and discuss the experimental aspects of this phenomenon in weak boson production processes.

In the works related to the analysis of the unified theories of the electromagnetic and weak interactions it was pointed out that there was a connection between the values of the magnetic moment of the vector-bosons and possible structures of these theories [1], [2]. In the early days of the SM, the processes pp ($p\bar{p}$) $\rightarrow W^\pm + \gamma + X$ were suggested for the measurement of the magnetic moment of the W boson, where the radiation amplitude zero was encountered first [3]. We discuss this zero in Section II. The observed zeros of these production processes belong to the so-called TYPE I zeros. We consider the conditions which have to be fulfilled in order that TYPE I radiation zeros can occur in Section III. We describe how these radiation zeros can be explained as a result of the factorization of the amplitudes as well as a consequence of the decoupling theorem. TYPE I zeros have two different

forms, *charge null zone* and *current null zone* zeros. We also give a few examples for the recently discovered TYPE II zeros. Section IV is devoted to the discussion of many interesting zeros, which occur in electroweak production processes. First, we discuss the zeros in $W\gamma$ and $W\gamma\gamma$ production. Here, we also briefly discuss the equalities of the values of the specific helicity amplitudes, which are responsible for the current null zone zeros. Next, we consider the WZ production zeros. Some of the WZ production amplitude zeros were observed only recently and they can not be attributed to any type of the zeros discovered earlier. Special attention is paid to a discussion of the full set of zeros in the WZ production process, since they directly relate to the zeros of two other production processes, the zeros in $q\bar{q} \rightarrow WZ\gamma$ and $q\bar{q} \rightarrow WZZ$, which are discussed subsequently. The amplitudes in the $W^\pm Z\gamma$ case have an especially rich structure in terms of zeros, revealing three different types of zeros. We also review the zeros in $WH\gamma$ production. The existence of the charge null zone requires the same sign for all the nonzero charges of the particles participating in the process and therefore processes, where only neutral electroweak gauge bosons are produced, can only exhibit the current null zone TYPE I zeros. We discuss several of these processes in terms of the radiation zeros together with the helicity amplitudes relations mentioned earlier in more detail at the end of this section. Finally, we present a summary table of the zeros, considered throughout Section IV.

II RADIATION ZEROS IN $W\gamma$ PRODUCTION

In this section we briefly discuss the radiation amplitude zeros phenomenon associated with the $p\bar{p} \rightarrow W^\pm + \gamma$ collision process¹ in order to illustrate several important theoretical and experimental features of this phenomenon. The parton level amplitudes responsible for this process exhibit zeros in the distribution of the scattering angle [3]. The position of the zero depends only on the charge of the quark (no helicity dependence):

$$\cos\theta = -(1 + 2Q_i) , \quad (1)$$

where θ is the angle between the W^- and the d quark, if one considers $d\bar{u} \rightarrow W^-\gamma$ process. Q_i is the electric charge of the quark in units of the proton charge e .

The value of $\cos\theta = -\frac{1}{3}$ (see Fig. 1a), obtained from Eq. (1), is in fact, characteristic for some other SM based process amplitudes too, as we will discuss later.

From the experimental point of view, the Tevatron collider ($p\bar{p}$) is especially well suited to observe the radiation zero predicted in $W\gamma$ production. See

¹⁾ For brevity, we will not write ‘+X’ addition, denoting backgrounds to the considered processes, hereafter.

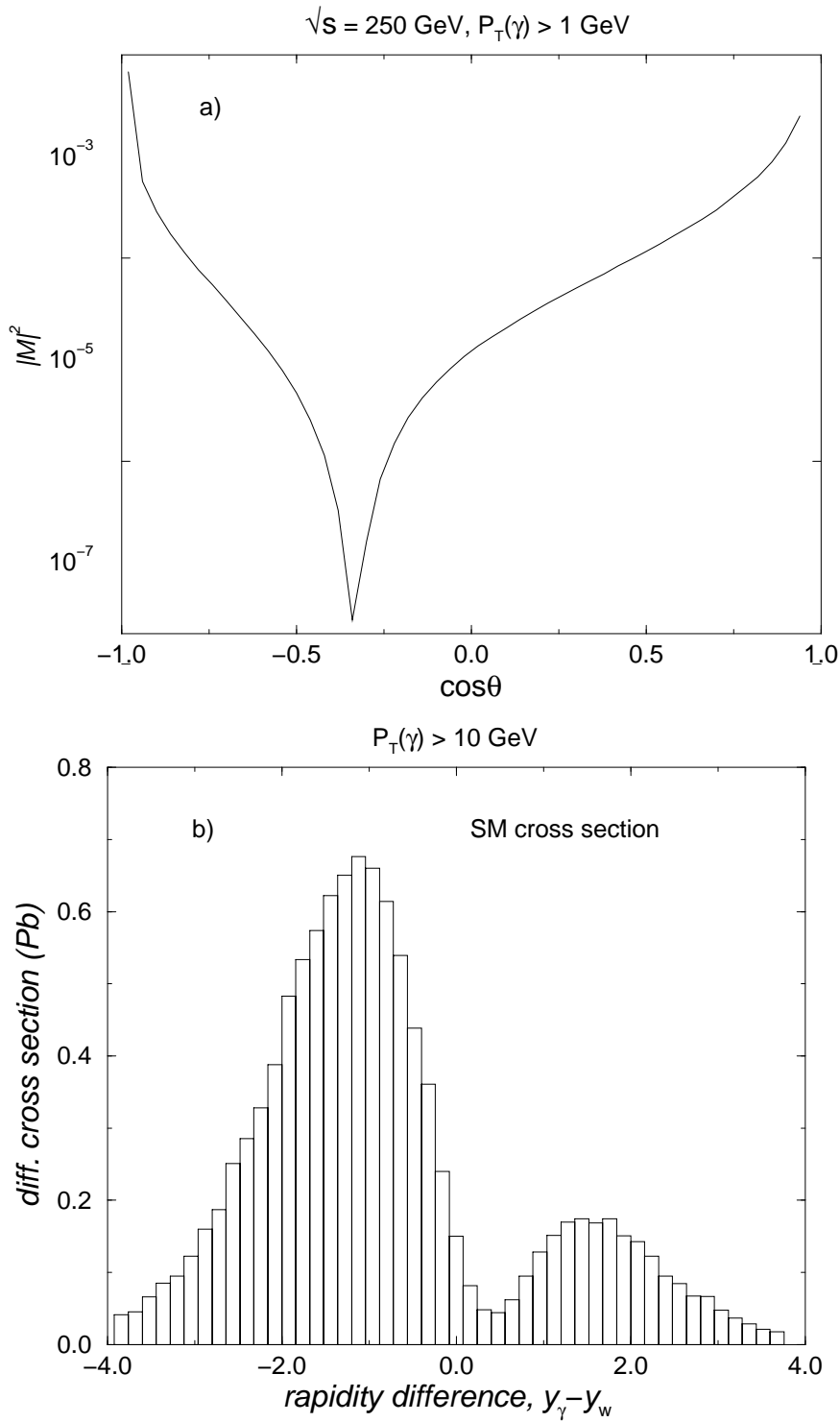


FIGURE 1. a) The zero in the angular distribution for $d\bar{u} \rightarrow W^-\gamma$ production for a center of mass energy of quark-antiquark system $\sqrt{s} = 250 \text{ GeV}$, b) Rapidity difference distribution for the $p\bar{p} \rightarrow W^-\gamma$ process at the Tevatron (2 TeV).

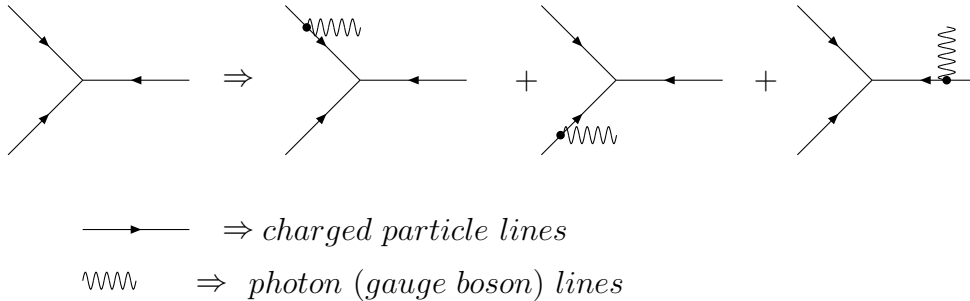
quark effects tend to wash out the dip caused by the radiation zero. At Tevatron energies, valence quark effects dominate and this effect is not a problem. As a result, the radiation zero leaves a clear signature. This is shown in Fig. 1b where we display the distribution² of the difference between the rapidities of the W boson, y_W , and the photon, y_γ . The dip at $y_\gamma - y_W \approx 0.3$ is due to the radiation zero [4].

The boost invariant quantity $y_\gamma - y_W$ contains the same information as the $\cos\theta$ distribution. The $y_\gamma - y_W$ distribution is very similar to the distribution of the rapidity difference between the photon and the charged lepton originating from the W decay, which can be readily observed. This is due to the $V - A$ nature of the W fermion antifermion coupling and the fact that W 's in $W\gamma$ production in the SM are strongly polarized: the dominant helicity of the W^\pm boson in SM $W^\pm\gamma$ production is $\lambda_W = \pm 1$ [4].

III RADIATION AMPLITUDE ZEROS AND GAUGE FIELDS

The amplitude zero observed in $W\gamma$ production belongs to the family of ‘TYPE I’ zeros which can be explained as a consequence of the factorization of the amplitude, shown soon after they were first discussed in the literature [5]-[8].

The scattering amplitude for the above mentioned process can be obtained starting from the vertex (source graph) which describes the interaction of the charged particles, attach a photon to each charged particle leg in turn and add all diagrams, as schematically depicted below:



One can show that the amplitude (for particles of any spin) can be written in the form

²⁾ We use histograms for the collider process distributions to distinguish them from the parton level curves and to get neat curves for the rapidity distributions at the relatively low Monte Carlo statistics. The histograms are also helpful to see the ‘bin structure’ of the numerical results for the differential cross sections. In all the graphs, not using the histograms, the horizontal axes are divided into fifty equal bins.

$$M_\gamma = \sum_i \frac{A_i B_i}{C_i} , \quad (2)$$

where A_i and B_i are factors which depend on the charge and polarization. C_i represent the particle propagators. This leads to the factorization of the amplitude into separately charge dependent and polarization dependent factors:

$$\sum_i \frac{A_i B_i}{C_i} = f(A_i, C_i) \cdot g(B_i, C_i) . \quad (3)$$

The factorization of the amplitudes holds for any ***gauge theory based vertex*** with no restriction on the number of particles, due to the relation between the photon (gauge boson) coupling and Poincare invariance. For the complete tree level amplitude for a source graph V_G consisting of a *single vertex* (no internal lines)

$$M_\gamma(V_G) = \sum \frac{Q_i J_i}{p_i \cdot q} , \quad (4)$$

where J_i are 'the vertex currents', arising from inserting the current j_i into the i^{th} leg of the vertex, with

$$j = j_{conv} + j_{spin} + j_{cont} + j_{YM} . \quad (5)$$

The convection current, $j_{conv} = p \cdot q$, corresponds to the first-order space-time translation of the given leg's wave function.

The spin current is a first-order Lorentz transformation of the wave function. For the Lorentz transformation

$$\Lambda_{\mu\nu} = g_{\mu\nu} + \lambda \omega_{\mu\nu} , \quad (6)$$

the spinor wave function ψ transforms as

$$\psi'(x') = S(\Lambda)\psi(x) , \quad (7)$$

where

$$\omega_{\mu\nu} = q_\mu \epsilon_\nu - \epsilon_\mu q_\nu , \quad (8)$$

λ is an infinitesimal length, $x' = \Lambda x$, and

$$S(\Lambda) = 1 - \frac{i}{4} \lambda \sigma_{\mu\nu} \omega^{\mu\nu} . \quad (9)$$

Therefore for a spinor

$$j_{spin} = \frac{i}{4} \lambda \sigma_{\mu\nu} \omega^{\mu\nu} . \quad (10)$$

The contact j_{cont} and Yang-Mills j_{YM} currents result from the transformations of the single derivative couplings and Yang-Mills vertices, correspondingly [5].

J_i depend on the polarizations, but not on the charges of the particles, and obey the identity

$$\sum J_i = 0 \quad (11)$$

as a result of Poincare and Yang-Mills symmetries [5].

Thus the vertex amplitude $M_\gamma(V_G)$ vanishes, if

$$\frac{Q_i}{p_i \cdot q} = \text{const} , \text{ for all } i . \quad (12)$$

The well-known ‘ $-\frac{1}{3}$ ’ zero occurring in $W\gamma$ production belongs to this type. The classical limit of these zeros is the vanishing of the dipole radiation for the system of particles with the same charge to mass ratio

$$Q_i/m_i = Q_1/m_1 , \text{ for all } i , \quad (13)$$

and giromagnet coefficients, g_i [5].

Since $\sum \delta_i Q_i = 0$, the amplitude $M_\gamma(V_G)$ will be zero, if

$$\delta_i \frac{J_i}{p_i \cdot q} = \text{const} , \text{ for all } i . \quad (14)$$

These zeros correspond to the *current null zone*. In the infrared limit, Eq. (14) reduces to

$$\frac{p_i \cdot \epsilon}{p_i \cdot q} = \text{const} , \text{ for all } i . \quad (15)$$

Since $p_i \cdot q \geq 0$ for all i , all the convection currents, $p_i \cdot \epsilon$, have to vanish in order that Eq. (15) will be satisfied. It is easy to see that this implies that all the charged particles are restricted to the plane (a line) perpendicular to the photon polarization vector $\vec{\epsilon}$ for a linearly (elliptically) polarized photon, in the c.m. frame. This is the quantum field theory analogue of the classical case that there is no electric dipole radiation perpendicularly polarized to the scattering plane.

The null zone conditions, Eq. (12) and Eq. (14) also imply the invariance under the replacements

$$\frac{Q_i}{p_i \cdot q} \rightarrow \frac{Q_i}{p_i \cdot q} + C \quad (16)$$

and

$$\frac{J_i}{p_i \cdot q} \rightarrow \frac{J_i}{p_i \cdot q} + C' , \quad (17)$$

respectively. Therefore, for a suitable choice of C and C' , the single vertex amplitude $M_\gamma(V_G)$ can be written as

$$M_\gamma(V_G) = \sum_{i \neq j, k} p_i \cdot q \left(\frac{Q_i}{p_i \cdot q} - \frac{Q_j}{p_j \cdot q} \right) \left(\frac{J_i}{p_i \cdot q} - \frac{J_k}{p_k \cdot q} \right) , \quad (18)$$

where the null zone conditions take an explicit form.

In the case of the source graphs with the internal lines (several source graphs), the tree radiation amplitude $M_\gamma(T_G)$ can be written as a sum over the vertices

$$M_\gamma(T_G) = \sum_v M_\gamma[V_G(v)] R(v) . \quad (19)$$

Here $R(v)$ is T_G less the vertex v . Each of $M_\gamma[V_G(v)]$ in Eq. (19) will have the same properties in terms of zeros as the single vertex amplitude $M_\gamma(V_G)$, Eq. (18) and therefore there exists a null zone under the condition Eq. (12) or Eq. (14), similar to the single vertex case.

From the conditions above we see that the null zones connect intrinsic (charge, spin) and space-time properties (Poincare transformation) of the particles involved. This makes it possible to use them in analysing the structure of the SM.

Radiation zeros can also be explained as a consequence of the decoupling theorem [9], [10]. The wave function of a system of particles in an external Yang-Mills field can be written as

$$\Psi(x) = ULT\chi(x) , \quad (20)$$

where $\chi(x)$ is the free solution of the field equations ($Q = 0$, no gauge boson emission), and ULT is the product of the local gauge (U), Lorentz (L), and displacement (T) transformations. The null zone condition

$$\prod_i (ULT)_i = 1 \quad (21)$$

leads to the charge null zone condition discussed above.

From the condition for the charge null zone we conclude that (since $p_i \cdot q \geq 0$)

$$\frac{Q_i}{Q_j} \geq 0 , \text{ for all } i, j . \quad (22)$$

Notice that the zeros will not necessarily be in the physical range of the parameters ($-1 \leq \cos \theta \leq 1$ in the case discussed here).

In $2 \rightarrow 2$ scattering processes, where one of the final particles is a massless neutral gauge boson, in the relativistic limit, the zeros occur at the angle

$$\cos \theta = \frac{Q_1 - Q_2}{Q_2 + Q_1}, \quad (23)$$

where Q_1 and Q_2 are the charges of the initial state particles.

For the reaction $d\bar{u} \rightarrow W^- \gamma$ we indeed get $\cos \theta = -\frac{1}{3}$, consistent with the result from a direct computation of the matrix elements.

One can also consider TYPE I zeros in supersymmetric extensions of the SM. The emission/absorption of the gauginos will also be associated with radiation zeros [11]- [13].

The presence of amplitude zeros requires a gyro-magnetic factor of $g = 2$. Any anomalous $WW\gamma$ coupling changes the value of g and destroys the radiation zero [5], [14], [15].

Recently another type of the zeros (TYPE II) was discovered ([16]- [18]) in the physical phase space range for the processes

$$e^+u \rightarrow e^+u + \gamma, \quad e^+d \rightarrow e^+d + \gamma, \quad (24)$$

and

$$q\bar{q} \rightarrow W^+W^- \gamma. \quad (25)$$

TYPE II zeros occur only if the emitted photons are located in the scattering plane. The theory, revealing the underlying symmetry of the production process amplitudes responsible for this zero has yet to be offered.

IV AMPLITUDE ZEROS IN WEAK BOSON PRODUCTION PROCESSES

In this section we discuss, somewhat systematically, the amplitude zeros exhibited by electroweak production processes³. We also show that the current null zones can be considered as a consequence of the equality of the specific helicity amplitudes. QCD corrections are expected to give noticeable contributions to the distributions. However, we do not consider them in this work, since the objective of our analysis is to investigate the important aspects of the radiation amplitude zeros phenomenon for the weak boson production amplitudes. MadGraph [19] was used in the analysis of the production amplitudes.

In our calculations we have used $M_W = 80.35$ GeV, $M_Z = 91.18$ GeV, $M_H = 150.0$ GeV for the W boson, Z boson and Higgs masses, respectively. The values of the coupling constants were taken at the W boson mass scale:

$$\alpha(M_W) = 1/128. \quad (26)$$

³⁾ For more details of the zeros, analyzed in the earlier works, see references at beginning of their discussions.

A $W\gamma$, $W\gamma\gamma$ production zeros

Besides the ‘ $-\frac{1}{3}$ ’ zeros discussed in Section II, the $q\bar{q}' \rightarrow W\gamma$ amplitudes also exhibit current null zone zeros [20], [21]. The amplitudes vanish *for all angles* within the SM, when the W boson is longitudinally polarized and the photon polarization vector $\vec{\epsilon}$ is perpendicular to the scattering plane in the c.m. frame. $W\gamma$ production as well as several other weak boson production processes exhibit another type of the current null zone at the 90° scattering angle. We will not discuss those zeros here. The complete description of them can be found in [21].

A radiation zero can occur not only when one massless neutral gauge boson is emitted, but also if two or more are radiated, provided that the neutral gauge bosons are all collinear [5], [15]. This is in agreement with the charge null zone condition, Eq. (12), since for the neutral gauge boson, $Q = 0$ and $p \cdot q = 0$ due to its collinearity to the photon (the second neutral gauge boson), and therefore there is no explicit violation of the condition. Here Q and p are the charge and momentum of the neutral gauge boson, respectively. The zero is located at the same scattering angle as in the case where only one boson is radiated. The charge null zone zero of $W\gamma\gamma$ production is illustrated in Fig. 2a, where we show the squared amplitude as a function of the photon scattering angle for $W\gamma\gamma$ production at $\sqrt{s} = 300$ GeV [22]. A $p_T(\gamma) > 5$ GeV cut has been imposed to avoid the infrared singularities associated with photon emission. The zero gradually vanishes for increasing values of the angle between the two photons. Nevertheless, there is a clear dip in the rapidity difference $y_{\gamma\gamma} - y_W$ distribution due to this zero for

$$\cos \theta_{\gamma\gamma} > 0 , \quad (27)$$

as shown in Fig. 2b, where $\theta_{\gamma\gamma}$ is the angle between the two photons in the c.m. frame. We have imposed the following transverse momentum and rapidity cuts on photon [23]:

$$p_T(\gamma) > 10 \text{ GeV} , \quad |y_\gamma| < 2.5 . \quad (28)$$

The helicity amplitudes for $W\gamma\gamma$ production are approximately equal in magnitude for all scattering angles and c.m. energies of the $W\gamma\gamma$ system for the following combinations of helicities

$$M(\lambda_W = 0, \lambda_\gamma = -1, \lambda_\gamma = -1) \approx M(\lambda_W = 0, \lambda_\gamma = 1, \lambda_\gamma = 1) , \quad (29)$$

where λ_W and λ_γ are the W boson and photon helicities. Because of the different values of both photon helicities, these amplitudes cannot be combined into the polarization amplitudes, and there is no current null zone in the $W\gamma\gamma$ production case. We will discuss this situation in more detail for $Z\gamma\gamma$ production case, where these equalities become exact.

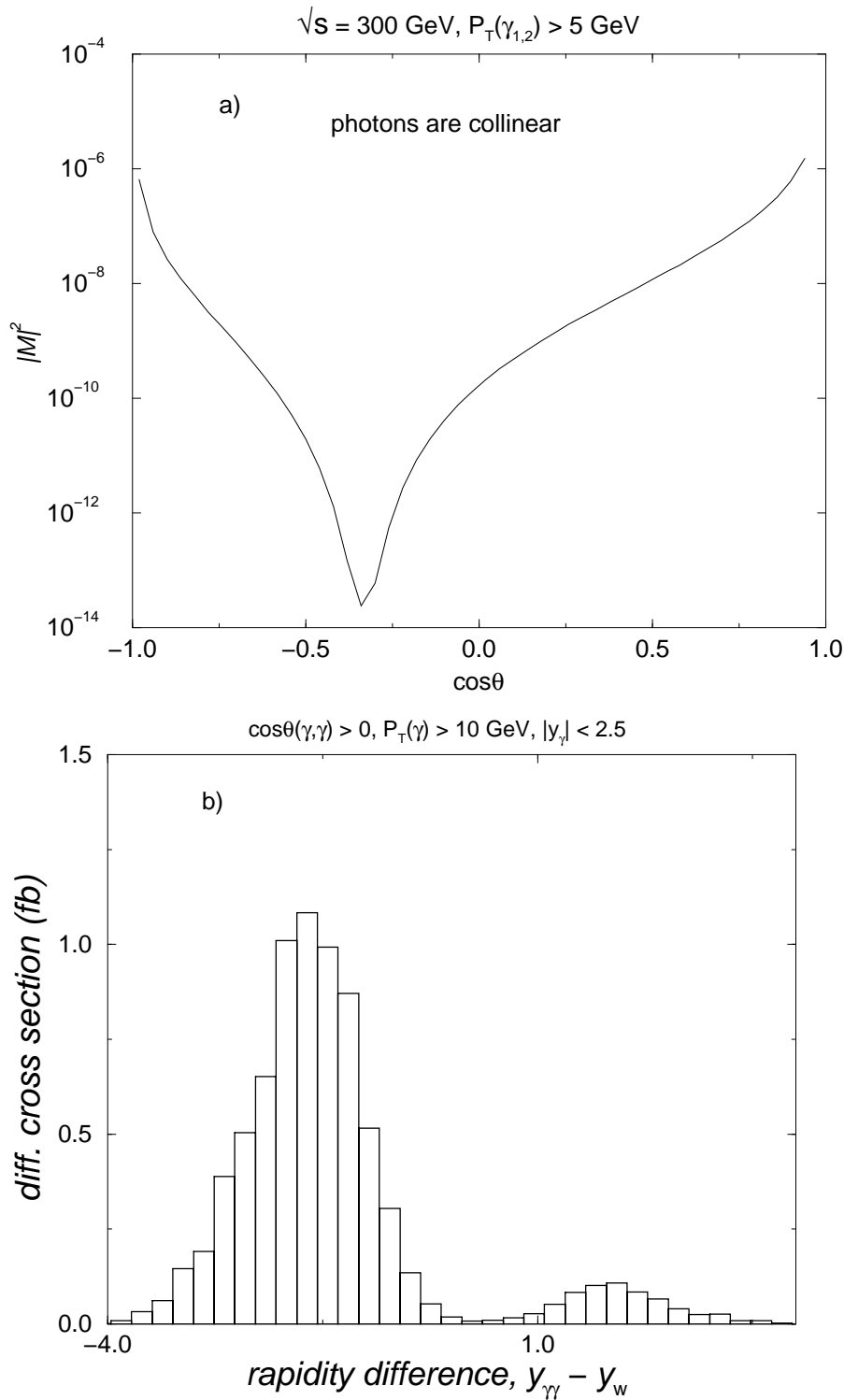


FIGURE 2. a) Radiation zero occurring in $d\bar{u} \rightarrow W^- \gamma\gamma$ production, b) The $y_\gamma - y_W$ rapidity difference distribution for $\cos\theta(\gamma,\gamma) > 0$ in $W\gamma\gamma$ production at the Tevatron.

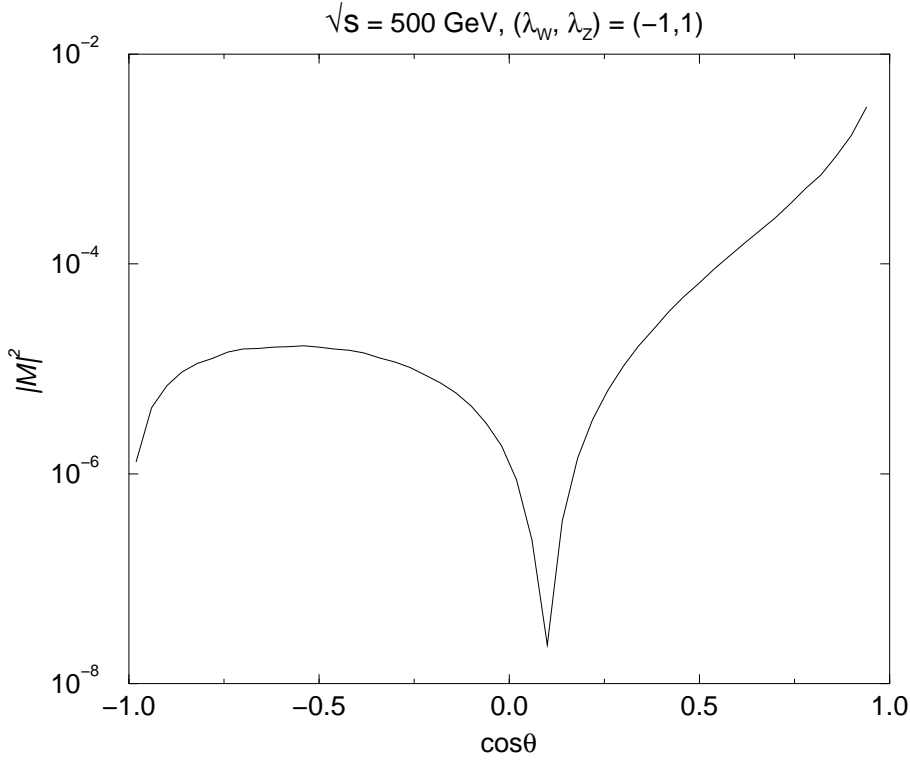


FIGURE 3. Amplitude zero in $d\bar{u} \rightarrow W^- Z$ production.

B WZ production amplitude zeros

In the case of massive neutral gauge bosons, the production amplitudes can still exhibit an approximate radiation zero [24], [25]. For the process

$$q_1 \bar{q}_2 \rightarrow WZ \quad (30)$$

the $M(\lambda_W = \pm, \lambda_Z = \mp)$ helicity amplitudes factorize into the helicity dependent term and the term, which depends on the weak boson fermion couplings (charge dependence), but not on the helicities of the particles (see [24] for more details). These amplitudes exhibit weakly energy dependent zeros, which at high energies, $\sqrt{s} \gg M_{W,Z}$, are located at

$$\cos \theta = (g_-^{q_1} + g_-^{q_2}) / (g_-^{q_1} - g_-^{q_2}), \quad (31)$$

where the $g_-^{q_i}$ ($i=1,2$) are the left-handed couplings of the Z boson to quarks and θ is the center of mass scattering angle of the W boson. Fig. 3 shows the $d\bar{u} \rightarrow W^- Z$ squared helicity amplitude for $\lambda_W = -1$ and $\lambda_Z = +1$. The processes

$$e^- \bar{\nu}_e \rightarrow W^- Z, \nu_e e^+ \rightarrow W^+ Z \quad (32)$$

also have similar zeros, as expected.

There are additional WZ production amplitude zeros, which are spin and energy dependent. The energy dependence is especially strong around the WZ threshold. Most of these zeros are located in the physical range of variables. We located the positions of the zeros both using *MATLAB*, algebraically, using explicit expressions for the amplitudes, and from the plots, $|M|^2$ vs $\cos \theta$ (for the values of the $\cos \theta$ in the physical region, $|\cos \theta| \leq 1$). In Fig. 4 we show several zeros of this type. Some of these zeros are approximately symmetric in $\cos \theta$ for the most part of the c.m. energy range (see Fig. 5) and leave two symmetric dips in the rapidity distributions for $PP \rightarrow W^- Z$. This occurs because two types of parton level contributions (d quark (beam 1) + \bar{u} quark (beam 2) and d quark (beam 2) + \bar{u} quark (beam 1) act coherently in terms of these zeros. Here ‘beam 1’ and ‘beam 2’ written in the parentheses show from which of two LHC proton beams the particular quark originates.

These zeros also leave deep dips in the rapidity distributions in the case of other helicity amplitudes, provided that they are relatively weakly energy dependent, so that the region of the dip in the $|M|^2$ vs $\cos \theta$ distribution due to the amplitude zero contains the value of $\cos \theta = 0$ for all important values of the c.m. energy. The $(\lambda_W = -1, \lambda_Z = 0)$ amplitude (Fig. 4) is an example for this case⁴.

The rapidity difference $y_Z - y_W$ distributions at the LHC for these two helicity combinations of particles are shown in Fig. 6.

C Zeros in $WZ\gamma$, WZZ and $WH\gamma$ production

In $WZ\gamma$, WZZ and $WH\gamma$ production all the nonzero charges have the same sign (see Eq. (22)) and all three processes include at least one neutral gauge boson. Therefore one expects the existence of charge null zones for these processes. As we shall demonstrate in the following, all these processes exhibit zeros in the physical range of variables.

The zeros of the $d\bar{u} \rightarrow W^- Z\gamma$ production process amplitudes are especially interesting, as the same helicity amplitude may have zeros originating from different sources.

Since it is not possible to write down a simple analytical expression for the squared matrix element in the general case (see Fig. 7 for the $WZ\gamma$ production Feynman diagrams), we try to identify the zeros near the threshold values of the center of mass energy of the $WZ\gamma$ system,

$$\sqrt{s} \approx M_W + M_Z, \quad (33)$$

⁴) More than 90% of the cross section for the $PP \rightarrow W^- Z$ with $(\lambda_W = -1, \lambda_Z = 0)$ at 14 TeV originates from the parton level process $d\bar{u} \rightarrow W^- Z$, $(\lambda_W = -1, \lambda_Z = 0)$ with the c.m. energy $\sqrt{s} \leq 350$ GeV.

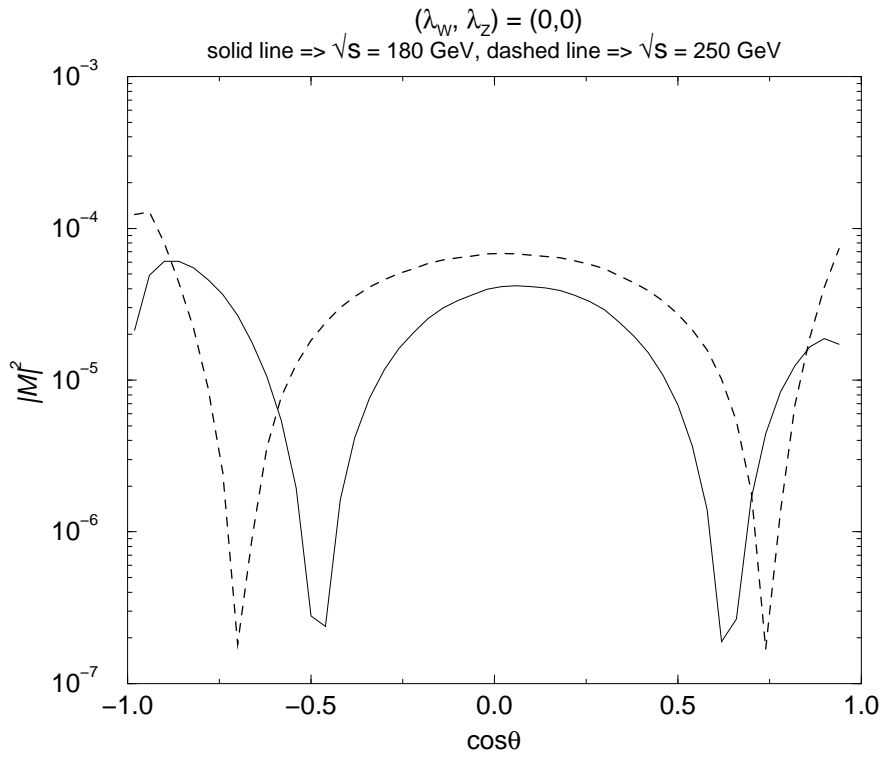
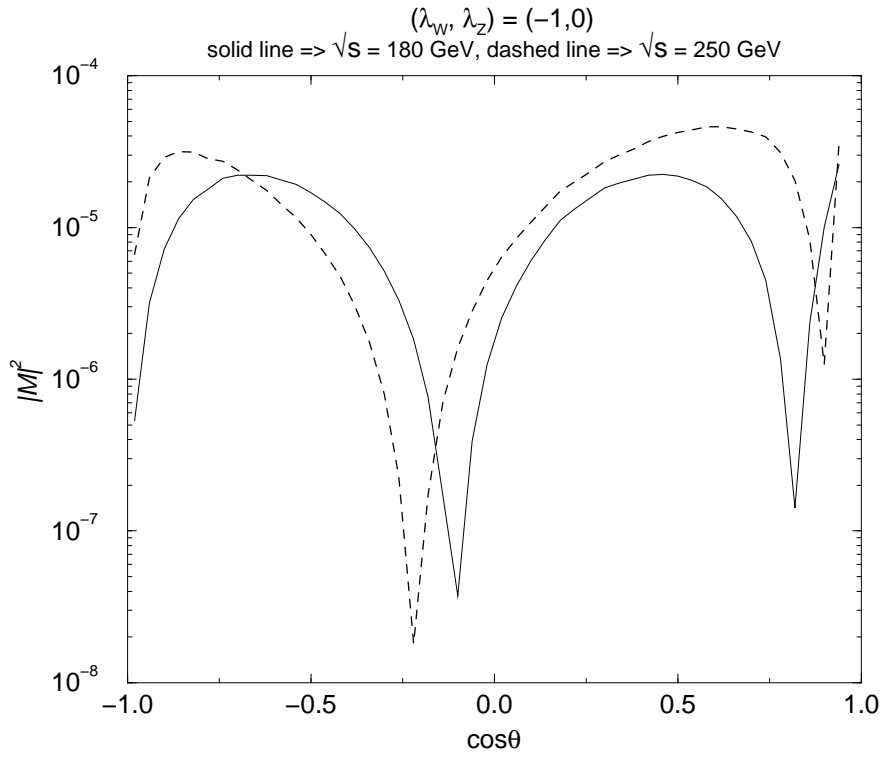


FIGURE 4. Zeros in $d\bar{u} \rightarrow W^- Z$ production for specific helicity amplitudes.

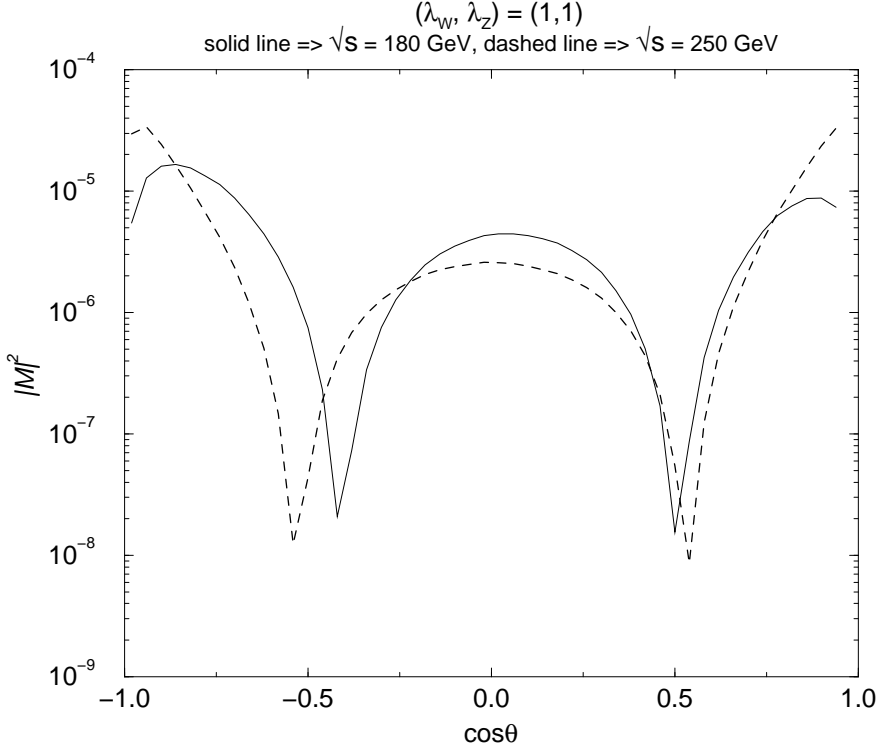


FIGURE 5. The squared $(\lambda_W, \lambda_Z) = (1, 1)$ amplitude as a function of the scattering angle in the $d\bar{u} \rightarrow W^- Z$ production .

where this can readily be done [18]. In this limit the photon momentum is small compared to the initial fermion (quark) momenta and therefore can be neglected in the numerators of the internal fermion propagators. It will be clear from the formulas below that if we choose the gauge, where transversely polarized (physical) photons have no 4th component, we can also neglect the contribution of the $WZ\gamma$ vertex to the amplitude, as both W boson and photon 3-momenta are very small. Under these conditions the $W^- Z\gamma$ production amplitude can be written as

$$M(W^- Z\gamma) = (-e)M(W^- Z)\epsilon_\mu^*(k_\gamma)j^\mu , \quad (34)$$

where j^μ is given by

$$j^\mu = Q_d \frac{p_d^\mu}{p_d \cdot k_\gamma} + (-1 - Q_d) \frac{p_{\bar{u}}^\mu}{p_{\bar{u}} \cdot k_\gamma} - \frac{k_W^\mu}{k_W \cdot k_\gamma} . \quad (35)$$

Here we considered the incoming quarks massless and used the Dirac equation to simplify the expression for j^μ . Since the 4th component of the W boson momentum ($\approx M_Z$) is not small, we keep k_W^μ in Eq. (35).

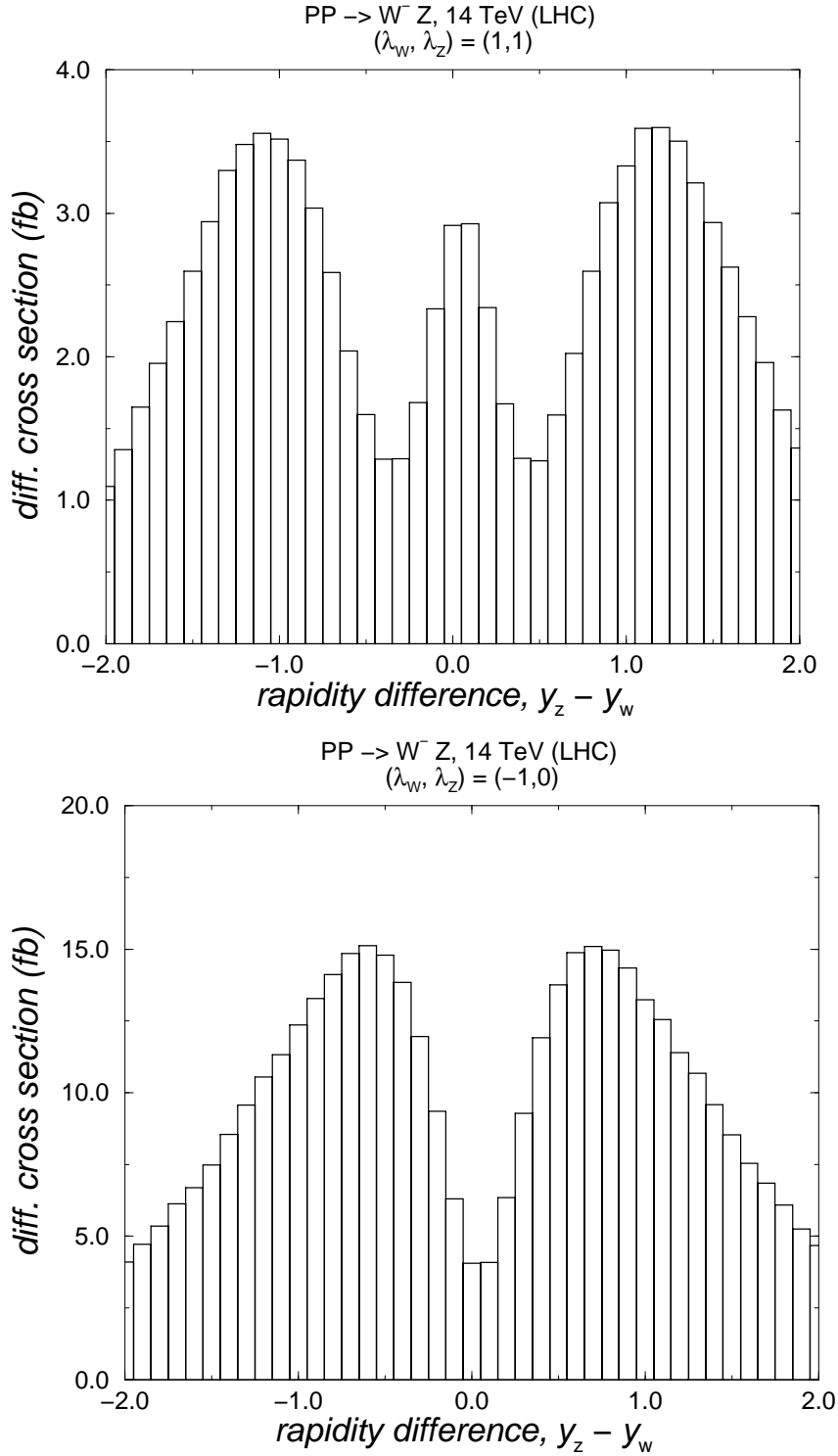


FIGURE 6. The $y_z - y_w$ distribution for the $(\lambda_W, \lambda_Z) = (1, 1)$ and $(\lambda_W, \lambda_Z) = (-1, 0)$ helicity amplitudes in $PP \rightarrow W^- Z$ at the LHC.

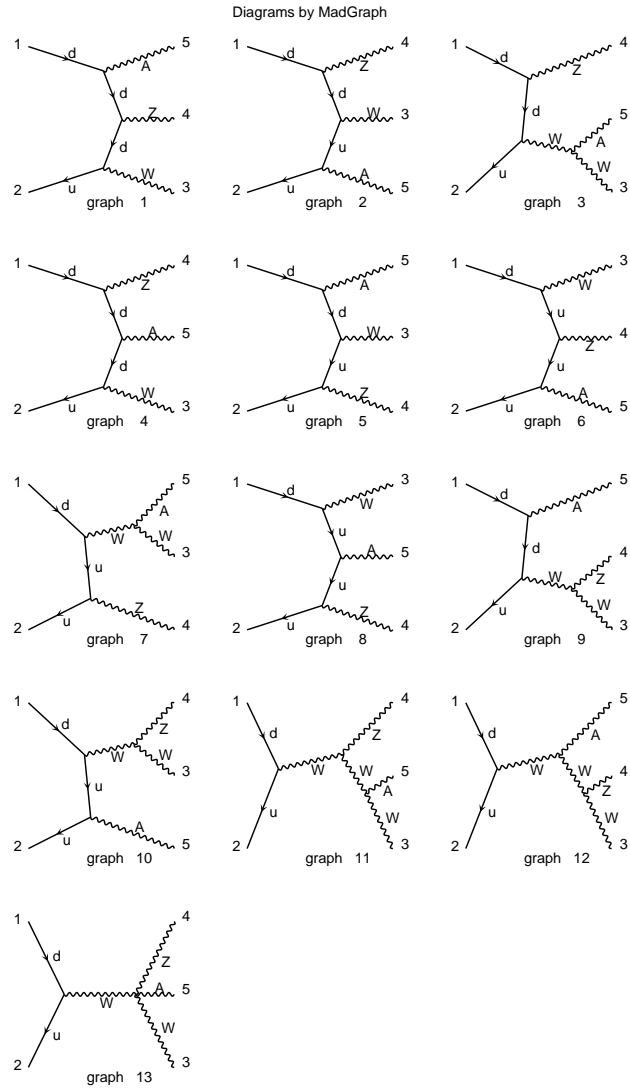


FIGURE 7. $WZ\gamma$ production Feynman diagrams generated by MadGraph.

The condition

$$\epsilon_\mu^*(k_\gamma)j^\mu = 0 \quad (36)$$

gives the zero of the amplitude at $\cos \theta_\gamma = \frac{1}{3}$, where θ_γ is the angle between the incoming d quark and the photon. To see this, one can choose

$$p_d = (E, 0, 0, E), \quad p_{\bar{u}} = (E, 0, 0, -E), \quad k_\gamma = E_\gamma(1, \sin \theta_\gamma, 0, \cos \theta_\gamma), \quad (37)$$

$$\epsilon_1^\mu = (0, 0, 1, 0), \quad \epsilon_2^\mu = (0, -\cos \theta_\gamma, 0, \sin \theta_\gamma). \quad (38)$$

Then

$$\epsilon_\mu^*(k)j^\mu = -Q_d \frac{\sin \theta_\gamma}{1 - \cos \theta_\gamma} + (-1 - Q_d) \frac{\sin \theta_\gamma}{1 + \cos \theta_\gamma} = 0 \quad (39)$$

or

$$\cos \theta_\gamma = 1 + 2Q_d = \frac{1}{3}.$$

In the case when the Z boson and photon are collinear,

$$\cos \theta_W = \cos(\theta_\gamma + \pi) = -\frac{1}{3}. \quad (40)$$

It is interesting to notice that the $\cos \theta_\gamma$ distribution will have a zero in this limit, even if the Z and γ are not collinear⁵, whereas the $\cos \theta_W$ distribution exhibits the zero only if the Z and γ are collinear. Now it is clear that any other zero(s) should come from the first term, i.e. from the $M(W^-Z)$ amplitude. Let's take, for example, the amplitude for $(\lambda_W, \lambda_Z, \lambda_\gamma) = (0, -1, -1)$. The squared amplitude vs $\cos \theta_W$ for the near the threshold value of the c.m. energy is given in Fig. 8. We also show the WZ production amplitude for $(\lambda_W, \lambda_Z) = (0, -1)$ in this figure. From the figure we see that, indeed, the WZ amplitude exhibits zeros at exactly the same locations as the $WZ\gamma$ amplitude. By requiring that the Z and γ are collinear, it can be seen that that '- $\frac{1}{3}$ ' zeros (dips) are energy (\sqrt{s}) and spin independent. The positions of the zeros in the WZ amplitudes and the corresponding zeros in the $WZ\gamma$ amplitudes also remain the same at the increasing values of \sqrt{s} for the collinear Z and γ .

In the case when the Z and γ are collinear, the total momentum of the $Z\gamma$ system is given by

$$\vec{p} = \vec{p}_Z + \vec{p}_\gamma = (1 + \alpha)\vec{p}_Z, \quad (41)$$

where $\alpha = \frac{p_\gamma}{p_Z}$. On the other hand, the invariant mass of the system is

⁵) A similar situation occurs also in $d\bar{u} \rightarrow W^- \gamma \gamma$, even for a larger range of center of mass energies, due to the masslessness of the photon.

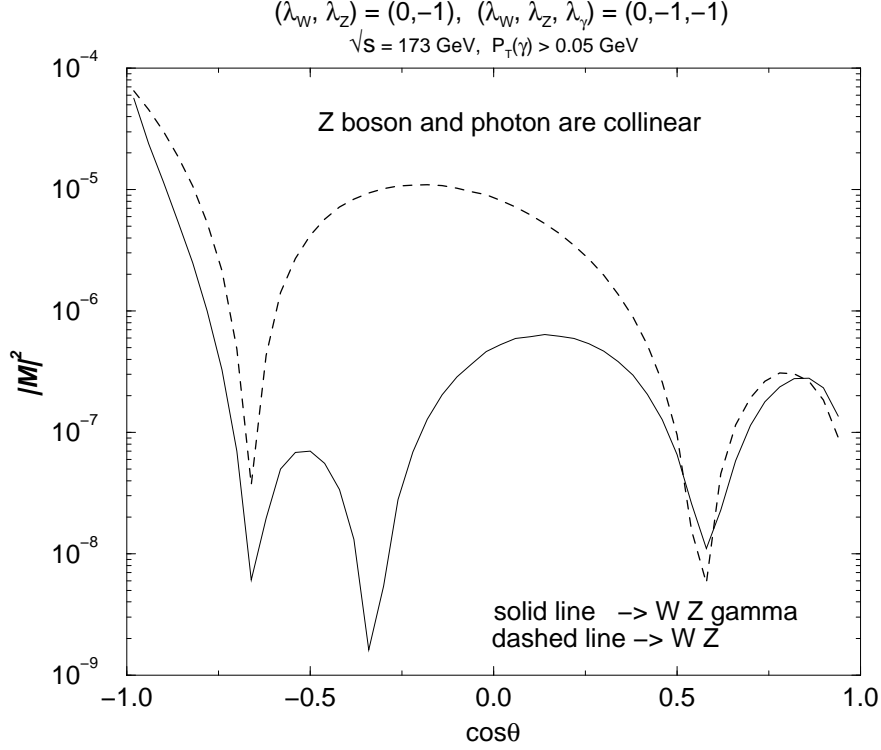


FIGURE 8. Zeros in $d\bar{u} \rightarrow W^-Z$ and $d\bar{u} \rightarrow W^-Z\gamma$ for a center of mass energy of $\sqrt{s} = 173$ GeV. Shown are the squared amplitudes for $(\lambda_W, \lambda_Z) = (0, -1)$ and $(\lambda_W, \lambda_Z, \lambda_\gamma) = (0, -1, -1)$. A $p_T(\gamma) > 0.05$ GeV cut has been imposed to avoid the infrared singularity present in $WZ\gamma$ production. The Z boson and the photon are collinear in the $WZ\gamma$ production case.

$$M_{inv} = (E_Z + E_\gamma)^2 - (\vec{p}_Z + \vec{p}_\gamma)^2 = M_Z^2 + 2\alpha p_Z \sqrt{M_Z^2 + p_Z^2} - \alpha p_Z^2. \quad (42)$$

By solving Eq. (41) and Eq. (42) together, we find

$$\alpha = \frac{-(Y^2 + Y p^2) \pm \sqrt{(Y^2 + Y p^2)^2 - Y^2(Y^2 - M_Z^2 p^2)}}{Y^2 - M_Z^2 p^2}, \quad (43)$$

where

$$Y = \frac{M_{inv}^2 - M_Z^2}{2}. \quad (44)$$

However, for this value of α , the momenta could be either collinear or opposite in direction, depending on whether the sign of α is positive or negative (see Eq.(41)).

We can remove the latter combination of p_Z and p_γ by requiring that

$$Y^2 - M_Z^2 p^2 \leq 0 \quad (45)$$

\sqrt{s}	173	200	250	300	350	400
M_{inv}^{max}	92.63	113.25	138.16	156.64	172.16	185.92

TABLE 1. The maximum invariant mass M_{inv}^{max} for the collinear Z boson and γ system at the different c.m. energies \sqrt{s} for $WZ\gamma$ production. All energy values are in units of GeV.

and it is clear that only the “-” solution of Eq. (43) should be used for the collinear case.

Eq. (45) can be transformed into a 4th order equation in M_{inv} and used to determine the upper limit of the invariant mass M_{inv} , when the Z boson and the photon are still collinear:

$$\left(1 - \frac{M_Z^2}{s}\right)M_{inv}^4 + 2\frac{M_Z^2 M_W^2}{s}M_{inv}^2 - M_Z^2 s - \frac{M_Z^2 M_W^4}{s} + 2M_Z^2 M_W^2 + M_Z^4 \leq 0 . \quad (46)$$

Here s is the squared center of mass energy of the $WZ\gamma$ system.

The solutions of Eq. (46) can readily be found by *MATLAB*. In table 1 we give the values of these upper limits for the invariant mass of the collinear $Z\gamma$ system, M_{inv}^{max} , at the different values of c.m. energy \sqrt{s} .

The other helicity amplitudes of $WZ\gamma$ production also have zero-rich structures. The amplitudes $(\pm 1, \mp 1, -1)$, $(\pm 1, \mp 1, +1)$ exhibit the earlier mentioned zeros of WZ production (see Eq. (31) and the text before it) and ‘ $-\frac{1}{3}$ ’ zero.

We would like to emphasize that the position of the ‘ $-\frac{1}{3}$ ’ dip may vary slightly and the depth of the dip may change substantially, depending on the transverse momentum cut of the photon and c.m. energy, revealing its approximate nature.

To summarize, the $WZ\gamma$ production amplitudes have a very rich structure of zeros originating from three different sources:

1. a radiation zero at $\cos\theta_\gamma = \frac{1}{3}$ connected with photon radiation,
2. the approximate radiation zero occurring in WZ production,
3. spin dependent zeros in some of the WZ production amplitudes discussed above.

The zero present at $\cos\theta_\gamma = \frac{1}{3}$ leads to a clear dip in the $y_{Z\gamma} - y_W$ rapidity difference distribution ($y_{Z\gamma}$ is the rapidity of the $Z\gamma$ system), if the cosine of the angle between the Z boson and photon is restricted to $\cos\theta(Z, \gamma) > 0$. The $y_{Z\gamma} - y_W$ distribution at the LHC is shown in Fig. 9.

The $WH\gamma$ production amplitudes also have a ‘ $-\frac{1}{3}$ ’ zero, if the Higgs boson H and γ are collinear (Fig. 10). The rapidity dip for $WH\gamma$ production distribution is not as prominent as in the $WZ\gamma$ case due to the lack of the

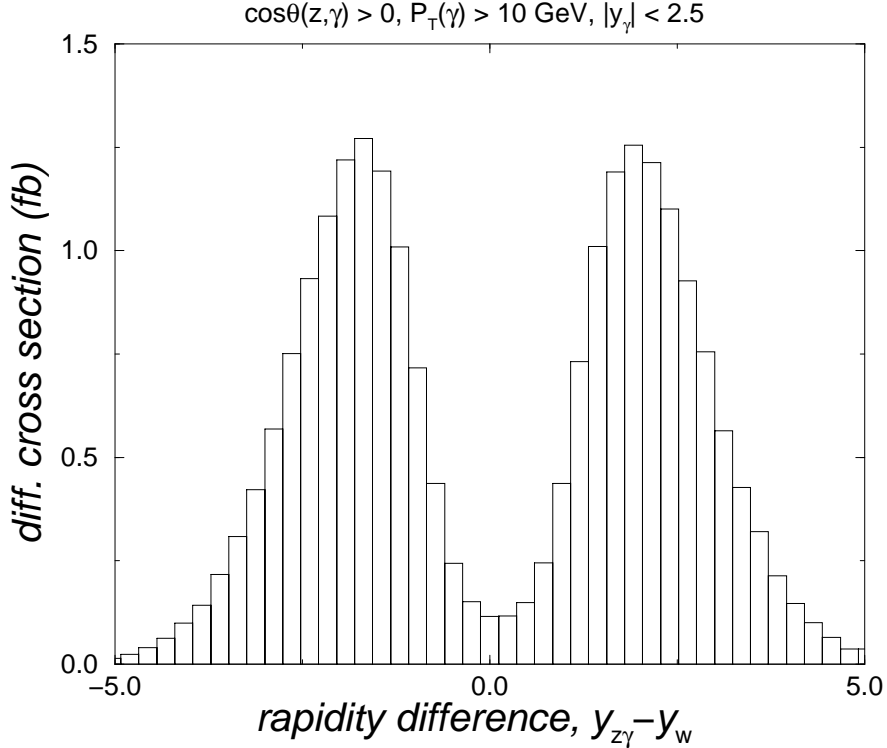


FIGURE 9. The $y_{Z\gamma} - y_W$ rapidity difference distribution for $\cos\theta(Z, \gamma) > 0$ in $WZ\gamma$ production at the LHC.

WZ zeros present in the $WZ\gamma$ helicity amplitudes⁶.

Similar to WZ production, the amplitudes for WZZ production exhibit an approximate radiation zero, if the two Z bosons are collinear (Fig. 11). The technique for generating collinear Z bosons is similar to that of the $Z\gamma$ ($H\gamma$) case with the only significant difference that both “-” and “+” solutions of the equation for α (see the text after Eq. (45)) can generate the collinear Z bosons. The amplitude zeros lead to a dip in the $y_{ZZ} - y_W$ distribution, which, however, is much less pronounced than the corresponding dip in the $y_{Z\gamma} - y_W$ distribution in $WZ\gamma$ production, due to the absence of the ‘ $-\frac{1}{3}$ ’ zero in the WZZ amplitudes. A comparison of the two distributions at the LHC is shown in Fig. 12. We only considered the contributions of the amplitudes, where the first two particles (W and Z) have the same helicities as the dominating helicity amplitudes of the WZ production, $(\lambda_W, \lambda_Z) = (\pm 1, \mp 1)$. There are four such amplitudes in the $WZ\gamma$ case and six amplitudes in the WZZ case. These amplitudes give a substantial part of the contributions to the total cross sections, while the rapidity difference distributions due to these amplitudes still exhibit clear dips without any restriction on the angle between the Z

⁶⁾ WH as well as ZH amplitudes do not exhibit amplitude zeros of any of the types considered in this section, as expected.

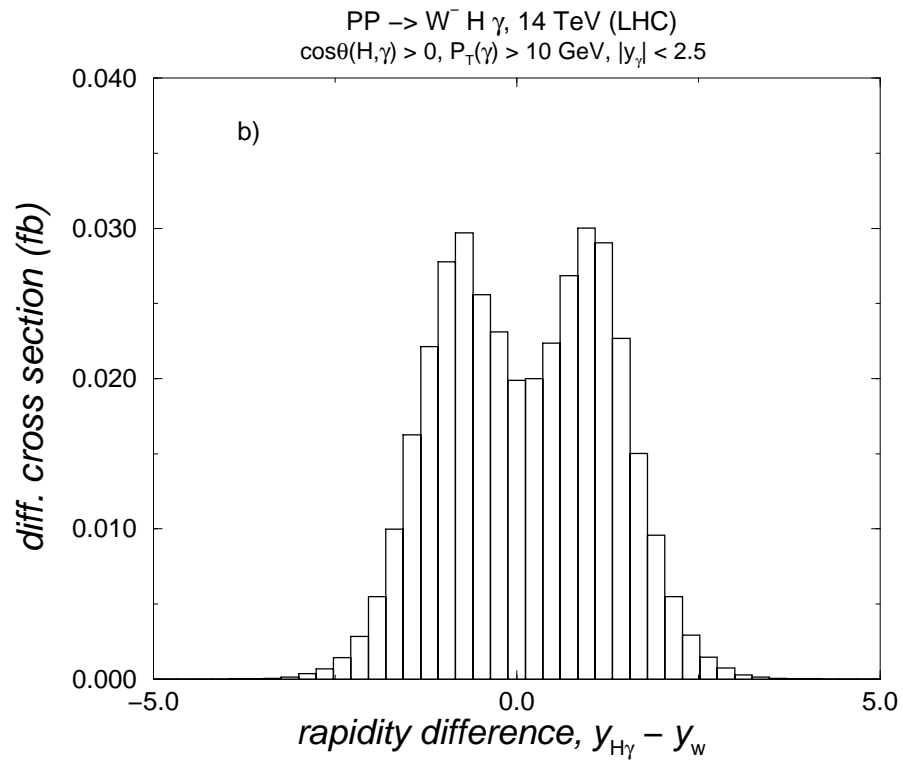
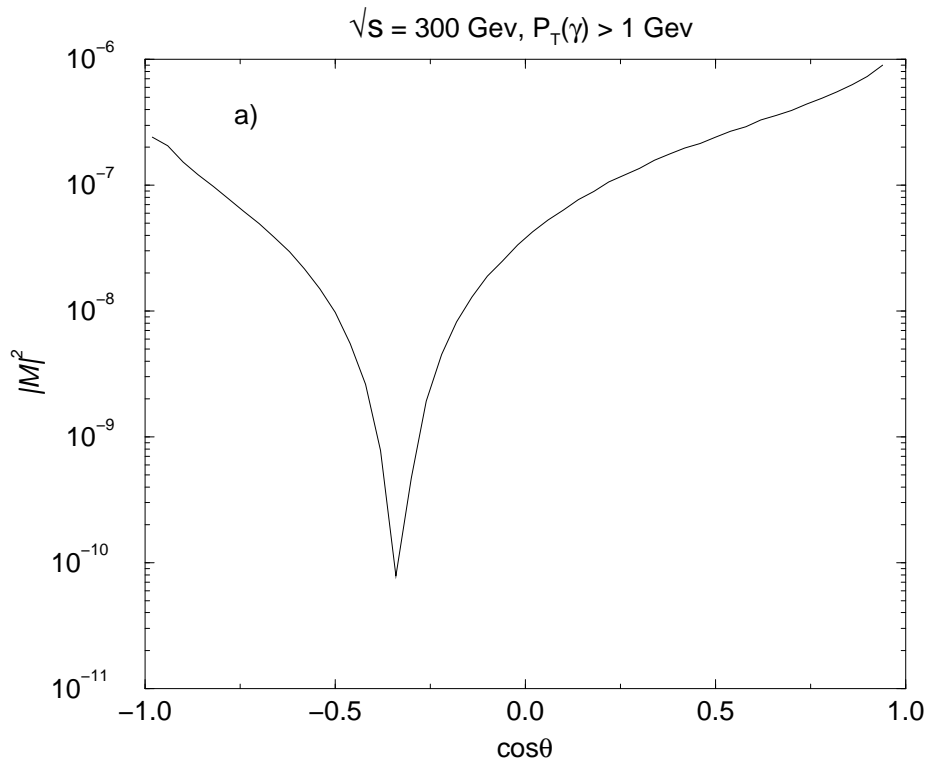


FIGURE 10. a) Zeros in $d\bar{u} \rightarrow W^- H \gamma$ production, b) The dip in the rapidity distribution in $PP \rightarrow W^- H \gamma$.

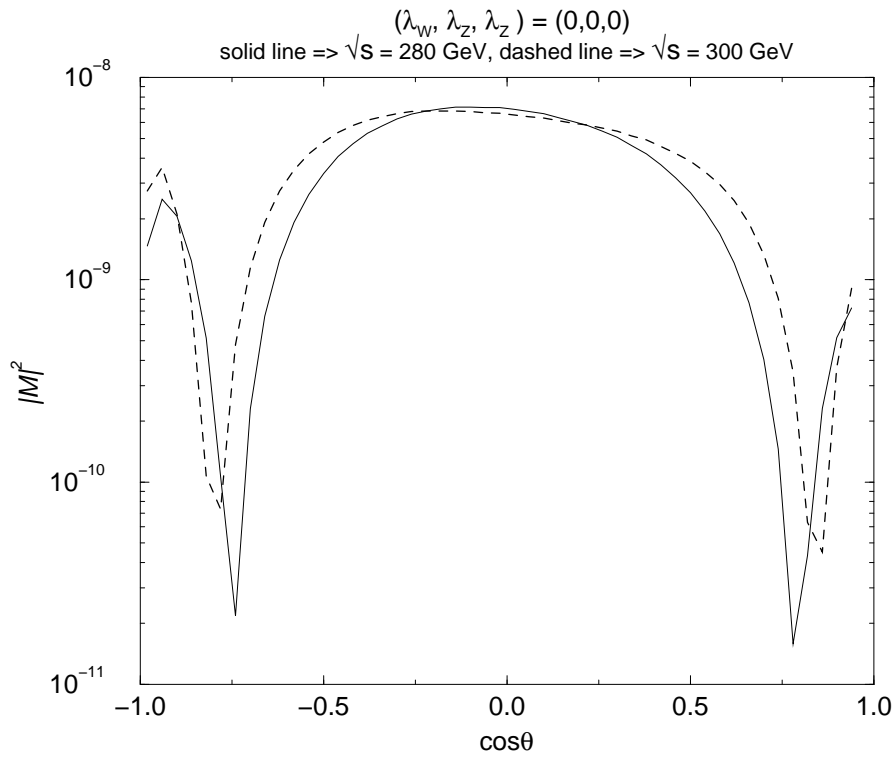


FIGURE 11. Zeros in $d\bar{u} \rightarrow W^- ZZ$ production. Shown is the amplitude with all three gauge bosons longitudinally polarized

boson and photon (the second Z boson).

The amplitudes for none of these three production processes exhibit the current null zone zeros discussed in the $W\gamma$ case.

D Zeros in neutral electroweak boson production processes and the helicity amplitude relations

Since these processes require the initial particles to have charges of different sign, the possibility of a charge null zone is excluded in this case (see Eq. (22)). Nevertheless some of these processes, namely, $Z\gamma$, $ZH\gamma$ and $ZZ\gamma$ production exhibit the same current null zones as the $W\gamma$ production process. The amplitudes vanish *for all scattering angles* within the SM, when the Z boson is longitudinally polarized and the photon polarization vector $\vec{\epsilon}$ is perpendicular to the scattering plane in the c.m. frame. In the $ZZ\gamma$ case, these are the helicity amplitudes for which both of the Z bosons are longitudinally polarized.

The $ZH\gamma$ production amplitudes exhibit zeros only if H and γ are collinear, while the $ZZ\gamma$ production amplitudes will still have approximate current null zone zeros for nonzero values of the angle between H and γ .

The existence of the current null zones discussed above implies the identities for the helicity amplitudes. For example, the current null zone in $Z\gamma$ production is the result of the following equality of the helicity amplitudes,

$$M(\lambda_Z = 0, \lambda_\gamma = -1) = M(\lambda_Z = 0, \lambda_\gamma = 1) . \quad (47)$$

The two polarization amplitudes built out of these helicity amplitudes are

$$M(\lambda = 1) = \frac{i}{\sqrt{2}}(M(\lambda_Z = 0, \lambda_\gamma = 1) + M(\lambda_Z = 0, \lambda_\gamma = -1)) \quad (48)$$

and

$$M(\lambda = 2) = \frac{1}{\sqrt{2}}(M(\lambda_Z = 0, \lambda_\gamma = 1) - M(\lambda_Z = 0, \lambda_\gamma = -1)) . \quad (49)$$

The polarization amplitude $M(\lambda = 2)$ will have a zero value for all scattering angles due to Eq. (47), which is the current null zone of the $Z\gamma$ production process.

Similarly, the current null zone in $ZZ\gamma$ production is due to the helicity amplitudes $M(\lambda_Z = 0, \lambda_Z = 0, \lambda_\gamma = \pm 1)$ being equal.

The equality of different helicity amplitudes does not always lead to the existence of a current null zone. In the $Z\gamma\gamma$ case, one can show that

$$M(\lambda_Z = 0, \lambda_\gamma = -1, \lambda_\gamma = -1) = M(\lambda_Z = 0, \lambda_\gamma = 1, \lambda_\gamma = 1) \quad (50)$$

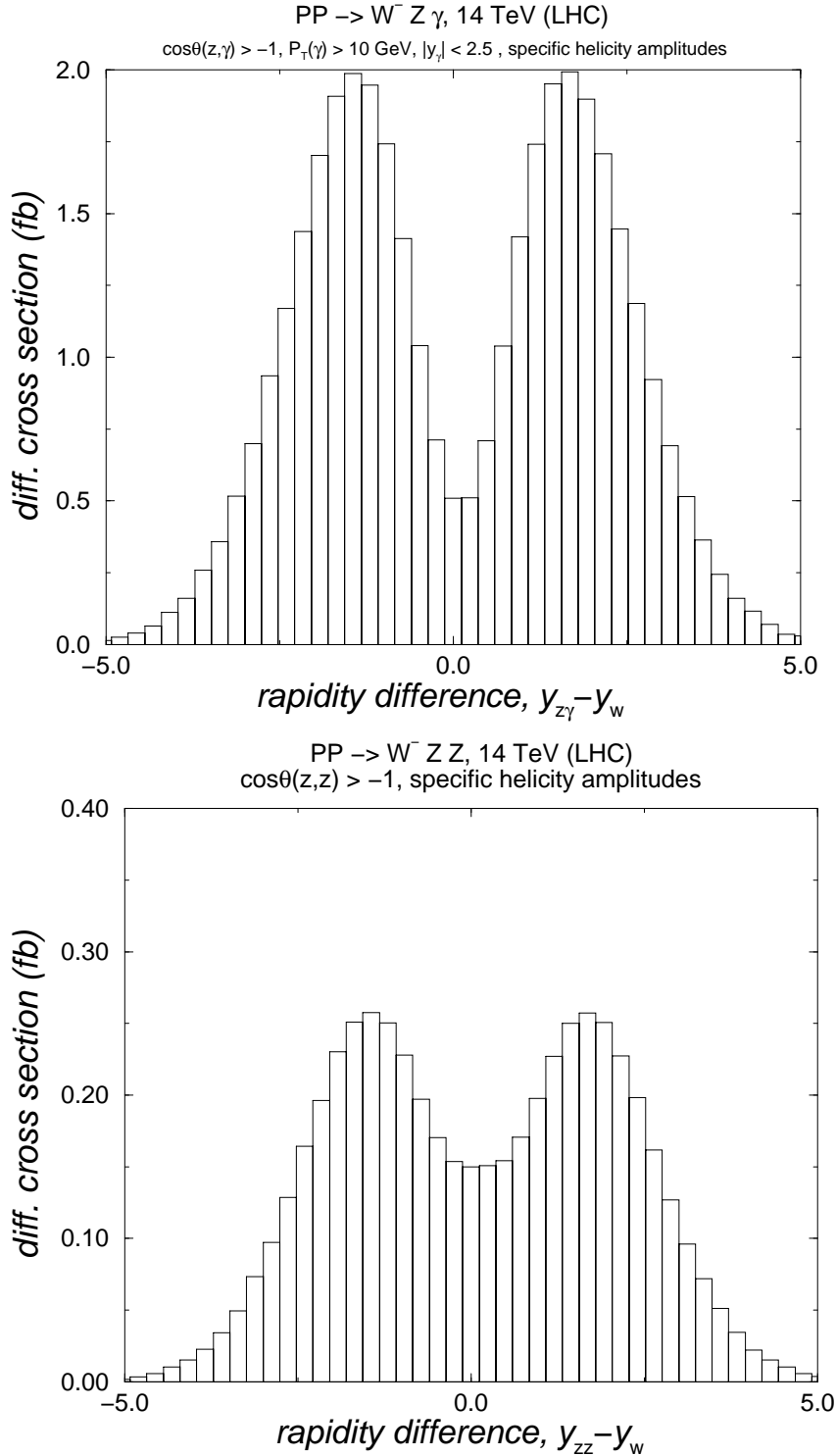


FIGURE 12. Comparison of the $y_{z\gamma} - y_w$ distribution in $WZ\gamma$ production, and the $y_{zz} - y_w$ distribution in WZZ production at the LHC. Contributions of the specific helicity amplitudes (see text) are considered.

and

$$M(\lambda_Z = 0, \lambda_\gamma = -1, \lambda_\gamma = 1) = M(\lambda_Z = 0, \lambda_\gamma = 1, \lambda_\gamma = -1) . \quad (51)$$

Similar to the $W\gamma\gamma$ case, since both photons have different helicities for these amplitudes, they cannot be combined into polarization amplitudes, one of which would have a zero value. Therefore, surprisingly, $Z\gamma\gamma$ production does not have a current null zone of the type found in the $Z\gamma$ and $ZZ\gamma$ cases.

The equality of the amplitudes with different particle helicities is also observed for the WW and ZZ production amplitudes:

$$M(\lambda_{W(Z)} = -1, \lambda_{W(Z)} = -1) = M(\lambda_{W(Z)} = 1, \lambda_{W(Z)} = 1) , \quad (52)$$

$$M(\lambda_{W(Z)} = 0, \lambda_{W(Z)} = -1) = M(\lambda_{W(Z)} = 1, \lambda_{W(Z)} = 0) . \quad (53)$$

Therefore, one can consider the current null zone, occurring at all scattering angles, as a special case of this equality of helicity amplitudes with different particle helicities, it occurs when the helicity of only one of the particles has different values for two amplitudes which are equal and it is therefore possible to combine the two amplitudes into the polarization amplitudes, one of which has zero value.

It is interesting that such a ‘classical’ process, as the two photon production process, for example, $u\bar{u} \rightarrow \gamma\gamma$, also exhibits the equalities of the amplitudes, and this occurs when all four particles have different helicities in two compared amplitudes:

$$M(\lambda_u = -1, \lambda_{\bar{u}} = 1, \lambda_\gamma(1) = -1, \lambda_\gamma(2) = -1) =$$

$$M(\lambda_u = 1, \lambda_{\bar{u}} = -1, \lambda_\gamma(1) = 1, \lambda_\gamma(2) = 1) , \quad (54)$$

$$M(\lambda_u = -1, \lambda_{\bar{u}} = 1, \lambda_\gamma(1) = -1, \lambda_\gamma(2) = 1) =$$

$$M(\lambda_u = 1, \lambda_{\bar{u}} = -1, \lambda_\gamma(1) = 1, \lambda_\gamma(2) = -1) , \text{ etc.} \quad (55)$$

In table 2 we present a summary of TYPE I null zones that we discussed in this section. We only included the current null zones that occur for all values of the scattering angle.

V CONCLUSION

The SM amplitudes for processes with the emission of one or more neutral gauge bosons exhibit zeros, the amplitudes vanish under the specific conditions. There are many different forms of zeros. The most investigated form of the zeros are TYPE I zeros. There are two forms of TYPE I zeros, the charge null zones and the current null zones. In the case of TYPE I charge

process	Charge null zone	Current null zone	Helicity amplitudes with equal values
$W\gamma$	+	+	+
$W\gamma\gamma$	+	-	+
WZ	+	-	-
$WZ\gamma$	+	-	-
$WH\gamma$	+	-	-
WZZ	+	-	-
$Z\gamma$	-	+	+
$ZH\gamma$	-	+	+
$Z\gamma\gamma$	-	-	+
$ZZ\gamma$	-	+	+
WW	-	-	+
ZZ	-	-	+
$\gamma\gamma$	-	-	+

TABLE 2. Charge null zone zeros, current null zone zeros and equalities of the helicity amplitudes exhibited by electroweak sector high energy processes within the SM in the physical region of parameters. ‘+’ (‘-’) sign corresponds to the presence (absence) of the null zone or of the helicity amplitudes with the equal values

null zones, the distributions of the scattering angles contain zeros. In the case of the TYPE I current null zones, either the amplitude completely vanishes or the distributions for the scattering angles contain zeros for certain helicity combinations of the particles. We briefly discussed the origin of TYPE I zeros, which are due to the factorization of the production amplitudes. The amplitudes can also vanish for many processes, when the photon (gauge boson) momentum is in the scattering plane created by the momenta of the other particles, which participate in the process. These zeros are called TYPE II zeros. Finally, there are those amplitude zeros, such as the recently observed zeros in WZ production, which could be just accidental zeros, due to the cancellations between the various terms in the amplitude. We have discussed all these different types of zeros and shown that some of the production amplitudes have an especially rich structure in terms of zeros. $WZ\gamma$ and WZZ production amplitudes are examples for this. Many of the zeros leave deep dips in the rapidity distributions, which could be observed experimentally. We also showed that the TYPE I current zones, occurring for all scattering amplitudes, are the special case of the equality of the values of the production (helicity) amplitudes for the specific helicity combinations of the particles.

ACKNOWLEDGMENTS

The discussions of the subject of this paper with U. Baur and A. Werthenbach were helpful. The author appreciates the discussion of the value of the

vector-boson magnetic moment with M. Veltman. The author would also like to thank R. Gonsalves for his valuable comments during preparation of this work for publication.

REFERENCES

1. T.D. Lee, C.N. Yang, *Phys. Rev.* **128**, 885-898 (1962).
2. K.J. Kim, Yung-Su Tsai, *Phys. Rev.* **D7**, 3710-3721 (1973).
3. K.O. Mikaelian, M.A. Samuel, and D. Sahdev, *Phys. Rev. Lett.* **43**, 746-749 (1979).
4. U. Baur, S. Errede, and G. Landsberg, *Phys. Rev.* **D50**, 1917-1930 (1994).
5. R.W. Brown, K.L. Kowalski, and S.J. Brodsky, *Phys. Rev.* **D28**, 624-649 (1983).
6. D. Zhu, *Phys. Rev.* **D22**, 2266-2274 (1980).
7. C.J. Goebel, F. Halzen, and J.P. Leveille, *Phys. Rev.* **D23**, 2682-2685 (1980).
8. S.J. Brodsky, and R.W. Brown, *Phys. Rev. Lett.* **49**, 966-970 (1982).
9. R.W. Brown, and K.L. Kowalski, *Phys. Rev.* **D30**, 2602-2607 (1984).
10. R.W. Brown, and K.L. Kowalski, *Phys. Rev. Lett.* **51**, 2355-2358 (1983).
11. V. Barger, R.W. Robinett, W.Y. Keung, R.J.N. Phillips, *Phys. Lett.* **B131**, 372-376 (1983).
12. R.W. Brown, and K.L. Kowalski, *Phys. Lett.* **B144**, 235-239 (1984).
13. D. DeLaney, E. Gates, O. Tornkvist, *Physics Letters* **B186**, 91-95 (1987).
14. R.W. Brown, *Vector Boson Symp. 1995*, 261-272.
15. R.W. Brown, M.E. Convery, and M. A. Samuel, *Phys. Rev.* **D49**, 2290-2297 (1994).
16. M. Heyssler, and W.J. Stirling, *Eur. Phys. J.* **C4**, 289-299 (1998).
17. M. Heyssler, and W.J. Stirling, *Eur. Phys. J.* **C5**, 475-484 (1998).
18. W.J. Stirling, A. Werthenbach, *Eur. Phys. J.* **C12**, 441-450 (2000).
19. T. Stelzer, W.F. Long, *Comput. Phys. Commun.* **81**, 357-371 (1994).
20. J. Cortes, K. Hagiwara, F. Herzog, *Phys. Rev.* **D28**, 2311-2313 (1983).
21. R.W. Brown, and K.L. Kowalski, *Phys. Rev.* **D29**, 2100-2104 (1984).
22. U. Baur, T. Han, N. Kauer, R. Sobey, and D. Zeppenfeld, *Phys. Rev.* **D56**, 140-150 (1997).
23. T. Han, R. Sobey, *Phys. Rev.* **D52**, 6302-6308 (1995).
24. U. Baur, T. Han, and J. Ohnemus, *Phys. Rev. Lett.* **72**, 3941-3944 (1994).
25. T. Han, *Vector Boson Symp. 1995*, 224-238.